Rubidium at high pressure and temperature

2000 J. Phys.: Condens. Matter 12 921

(http://iopscience.iop.org/0953-8984/12/6/314)

J. Phys.: Condens. Matter **12** (2000) 921–931. Printed in the UK PII: S0953-8984(00)02411-5

Rubidium at high pressure and temperature

Per Söderlind and Marvin Ross

Lawrence Livermore National Laboratory, University of California, Livermore, CA 94551, USA

Received 9 March 1999, in final form 29 November 1999

Abstract. In the present paper we report theoretical calculations for the Hugoniot of shock-compressed rubidium. We use an all-electron full-potential method based on density-functional theory to obtain the total energy, pressure and electronic density of states. Thermal contributions to the equation of state (EOS) were introduced through temperature dependent occupation of the electronic states and a Grüneisen model was used for determining the nuclear thermal motion. The calculated Hugoniot is in very good agreement with the shock experiments. A temperature of about 10 000 K is reached at the pressure of about 300 kbar, the highest reached experimentally. Rubidium was chosen for this study because it undergoes a sequence of unusual pressure-induced structural transitions which have been attributed to s–d electron transfer. Since most studies of s–d transfer have been carried out at temperatures below 500 K, little is known of how it effects the equation of state at very high temperature. We found that the predicted Rb Hugoniot is very sensitive to the thermal s–d electron transfer, which leads to a considerable lowering of the predicted Hugoniot pressure and temperature.

1. Introduction

High pressure diamond-anvil experiments supplemented by electron band calculations have now provided sufficient data to clearly demonstrate that s–d electron transfer is responsible for many of the pressure-induced structural transformations observed in the transition and rare-earth metals [1] and the heavy alkali and alkaline metals [1–3]. For example, in the case of the transition metals it has been shown that the structural sequence across the series, hcp $\rightarrow$ bcc $\rightarrow$ hcp $\rightarrow$ fcc can be related to the increase in d-electron occupation number as the energy bands become progressively filled [1]. The trivalent lanthanide metals from La to Lu, (excluding Ce, Eu and Yb) show a systematic sequence of phase transitions hcp $\rightarrow$ Sm-type $\rightarrow$ dhcp $\rightarrow$ fcc $\rightarrow$ distorted fcc that has been related to an increasing d character of the conduction band under pressure [3].

The physical origin of the s–d transfer has been found from electron band calculations. Because s-wave functions are more extended in space than d functions, compression induces the s-like states to rise in energy relative to the d-like levels leading to a transfer of s-like conduction electrons to d-states. Since the s-like levels rise in energy with compression they are more repulsive and this transfer is accompanied by a lowering of the pressure and an increase in the compressibility of the material. s–d electron transfer is now recognized as one of the most important guiding principles for understanding the high pressure states of the metallic elements.

It is generally agreed that s–d electron transfer can also be accomplished by increasing the temperature. However, virtually all of the experimental work to date on the s–d transition has been carried out at or near room temperature using diamond-anvil cells (DACs) so that there is

very little known experimentally about how thermal s–d transfer actually affects the equation of state.

Shock-wave experiments have proven to be a very important method for generating simultaneously very high pressures and temperatures. In a shock-wave experiment, a supersonic wave is passed through the material under investigation [4]. A measurement of the shock velocity and mass velocity are sufficient to determine the thermodynamic pressure, volume and energy (P, V, E) of the compressed state. The P, V and E behind the shock front are related to the initial properties (P_0, V_0, E_0) in front of the shock wave by the Hugoniot equation,

$$E - E_0 = \tfrac{1}{2}(P + P_0)(V_0 - V). \tag{1}$$

The resulting P–V curve is known as a Hugoniot and represents the locus of points that can be reached from an initial condition. However, temperature cannot be obtained directly from the Hugoniot but must either be measured by a separate diagnostic, usually by fitting the emitted radiation to a Planckian function, or determined from a calculation. The Hugoniot can be calculated for a given material by using equation (1) with a knowledge of the equation of state.

Of the metallic elements, the heavy alkali metals Rb and Cs are among the best suited for studying the effects of thermal electron excitation. These metals undergo a sequence of unusual structural transitions which have been attributed to s–d electron transfer [5, 6]. They are very compressible so that shock experiments lead to very high temperatures. In the case of Rb we estimate the temperature to be about 13 000 K ($kT \sim 1.1$ eV) near 300 kbar. For comparison, iron only reaches a temperature of 10 000 K when shock compressed to 4.0 Mbar [7]. Since alkali metal Fermi energies are of the order of 2 eV the high temperature generated in a shock experiment can be expected to thermally excite a large fraction of conduction electrons from s to d states. The relatively small Fermi energy and high compressibility of alkali metals suggests that these elements provide an optimum set of materials for studying the effects of temperature on the equation of state of metals.

Hugoniot measurements for shock-compressed Cs and Rb were reported by Rice in 1965 [8]. Of the two metals Rb is the more favourable case for further theoretical examination. The reason is that the s–d transition for caesium begins near atmospheric pressure and terminates near 100 kbar, and this pressure only marginally overlaps the lower range for which the shock technique becomes useful. In the case of Rb the s–d transition terminates near 400 kbar and thus provides the better candidate for further study.

In the present paper we report calculations of the Rb Hugoniot in which we use state of the art electron band theory methods to obtain contributions to the thermodynamic properties arising from the thermally excited electrons. The equation of state is calculated by the Grüneisen model, described in section 2. This section also includes the description and results of the full-potential linear muffin-tin method (FP-LMTO) band theory used to calculate a series of finite temperature static lattice isotherms. The results of the Hugoniot calculations are in section 3, and section 4 is the discussion. The results point out the need to explicitly include electronic thermal excitation in order to accurately describe the thermodynamic state of shock-compressed Rb.

2. The Grüneisen equation of state

The energy and pressure for shock compressed Rb were calculated using the Grüneisen model [9, 10], where

$$E(T, V) = E_{el}(T, V) + 3NkT \tag{2}$$

and

$$P(V, T) = P_{el}(T, V) + 3\gamma_n NkT/V. \tag{3}$$

$E_{el}(T, V)$ and $P_{el}(T, V)$ refer to the total energy and pressure of the finite temperature static lattice (omitting nuclear motion) calculated by the FP-LMTO method described below. The second terms in equations (2) and (3) are the thermal corrections arising from nuclear motion, where γ_n is the Grüneisen parameter.

2.1. The Grüneisen parameter

The Grüneisen parameter is defined as $\gamma_n = V(\partial P/\partial E)_v$ and was calculated from the Slater model [11],

$$\gamma_n = -\frac{2}{3} - \frac{V}{2}\left[\frac{\partial^2 P_L}{\partial V^2}\Big/\frac{\partial P_L}{\partial V}\right].$$

P_L is the static lattice pressure at 300 K. Strictly, P_L should be determined at $T = 0$ K but the difference can be shown to be negligible, particularly for the case of very high final shock temperatures.

The Grüneisen model is a simple approximation, but a reliable model for a thermodynamically self-consistent hot liquid s–d metal is not now available, and is unlikely to be for some time. However, to justify our particular use of the Slater model we show below, in figure 7, that in the region of interest both the Slater and the Dugdale–McDonald [4] approximations give almost identical results. Perhaps more important, both models approach the correct limiting case for a static lattice, $\gamma_n = 0.5$.

2.2. The full-potential linear muffin-tin method (FP-LMTO)

The electronic equation of state and electronic structure were calculated by the all-electron first-principles full-potential linear muffin-tin orbital (FP-LMTO) method. The method uses linear muffin-tin orbitals in the wave function expansions and the potential makes no shape approximation in the interstitial regions. The method is based on the local-density approximation (LDA) for the electron exchange and correlation energy of the electrons but in this work we have adopted a more modern and accurate version which also contains corrections originating from gradient terms of the electron density. This method is referred to as the generalized gradient approximation (GGA) [12]. The electron charge density and potential is determined by the process of minimizing the total energy.

The wave function is represented as an expansion of basis functions. Since the number of k points used in the calculation has to be finite we chose to use up to about 200 k points in the irreducible part of the Brillouin zone. Furthermore, all relativistic terms, including the spin–orbit coupling, are accounted for in the Hamiltonian.

The present method incorporates non-sphericity to the charge density and potential by representing the crystal with non-overlapping spheres (of a variable, optimum size) surrounding each atomic site and a general shaped interstitial region between the spheres. Hence, we deal with two types of geometrical region in the calculations. Inside the spheres, the wave functions are represented as Bloch sums of so-called linear muffin-tin orbitals and are expanded by means of structure constants. The kinetic energy is not restricted to be zero in the interstitial region and the wave function expansion contains Hankel and Neumann functions (depending on sign of the kinetic energy) together with Bessel functions.

In order to represent the wave functions in Rb as accurately as possible we have defined here, in a single energy panel, 4s and 4p semi-core states and 5s, 5p, 4d and 4f valence

states. The 'double-basis-set' approach has been used, i.e. two kinetic energy parameters κ^2 appropriate for the tails of the semi-core states, and the valence states have been used.

As in the case for iron [13], the total energy converges slowly with respect to the k-point sampling used in the appropriate summations over the Brillouin zone (BZ) at high pressures. Here we have used up to 204 k points in the irreducible (1/48th) part of the BZ. The 33 total energy points were then locally fitted in a least-squares manner using the Murnaghan equation-of-state form [14].

The total energy was calculated at 33 volumes for six different temperatures, 315, 2000, 4400, 8800, 17 600 and 25 000 K. The calculation is self-consistent. The thermally excited electronic structure is calculated from the Fermi–Dirac temperature distribution and the entropy is obtained from the density of states. The electronic entropy contribution is determined from the expression

$$S_{el}/k = -\int N(E)[(f)\log(f) + (1-f)\log(1-f)]\,\mathrm{d}E$$

where $N(E)$ and f are the electron density and the Fermi–Dirac function, respectively. The thermodynamic variables are then determined from the Helmholtz free energy, $A_{el} = E_{el} - TS_{el}$. These data are then introduced into the Grüneisen equation of state model.

2.3. Finite temperature FP-LMTO results

At ambient conditions rubidium stabilizes in the bcc structure. With increasing pressure the solid converts to fcc at 70 kbar and above 130 kbar goes through a transition leading to several new phases of undetermined structures [15]. As a result the higher pressure isotherm is not well known. Figure 1 shows the DAC isotherm curve obtained from the fits to data of Winzenick *et al* [15], and points calculated using the full-potential linear muffin-tin method (FP-LMTO). The agreement between experiment and theory is good up to the fcc–phase III transition at 130 kbar. Above this pressure the Hugoniot is already in the liquid phase and further comparisons with DAC studies are irrelevant. Of greater importance are the high temperature isotherms and the density of states.

Figure 2 shows a series of isotherms calculated for temperatures ranging from 300 to 25 000 K. The noteworthy feature is that with successively higher temperature, up to about 200 kbar, each isotherm has a lower pressure at a given volume. This unusual behaviour is a consequence of the s–d transition.

Figures 3(a)–(d) show the calculated density of states (DOS) for bcc rubidium at several successively smaller volumes. In our approach the l-projected DOS can only be obtained within the muffin-tin spheres. One cannot distinguish in these plots between, for example, 4s and 5s states. As a function of compression a small fraction of the electrons will leak out to the interstitial region with no specific l character. For Rb, however, the total leakage of core and valence electrons was rather small. At ambient pressure, about 0.5 electrons and at the highest pressure about one electron occupied the interstitial region.

At ambient conditions, figure 3(a), the electronic character is mainly s-like with a strong mix of p and d below the Fermi surface, but mainly d-like above the Fermi-surface. With compression the electronic character becomes increasingly d-like. This results in a highly compressible 0 K static lattice isotherm. The effect of temperature is to thermally excite electrons above the Fermi surface thereby increasing the overall d character and lowering the pressure. The DOS plots show that Rb becomes predominantly d-like in the pressure range above 300 kbar and further compression or thermal excitation can no longer change the electronic character. In other words the s–d transition is complete and as a result all the isotherms converge, as in figure 2. The effect of both compression and temperature is also

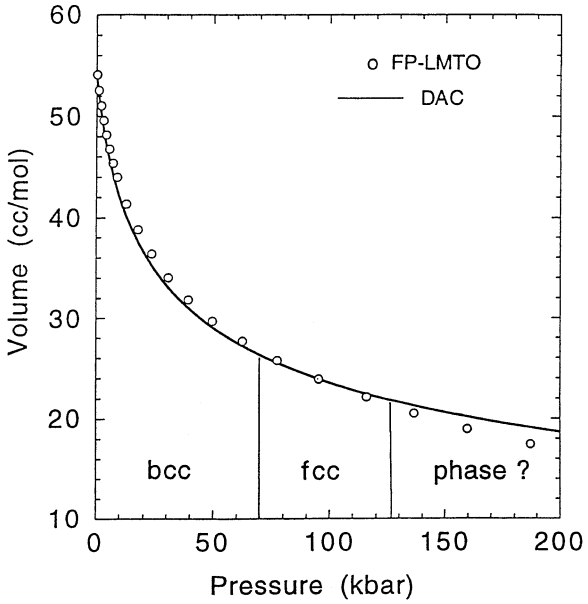

Figure 1. Rubidium isotherms. The full curve is the diamond anvil cell (DAC) room temperature isotherm plotted from the fits to data of Winzenick *et al* [15], and the circles are the calculated values obtained using the full-potential linear muffin-tin method (FP-LMTO).

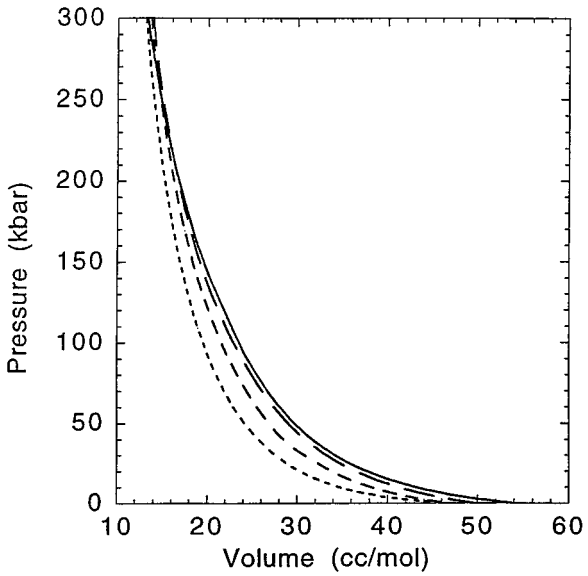

Figure 2. Isotherms calculated for temperatures ranging from 300 to 25 000 K. The highest pressure isotherm (full curve) is at 300 K. With decreasing pressure, but increasing temperature, are isotherms at 8800, 17 600 and 25 000 K (short-dashed curve).

shown in figure 4, the d occupation increasing at the expense of the s electrons with increasing compression. The effect of the higher temperatures is to transfer s electrons to d states for all but the most compressed volumes, where the temperature effect diminishes and even reverses.

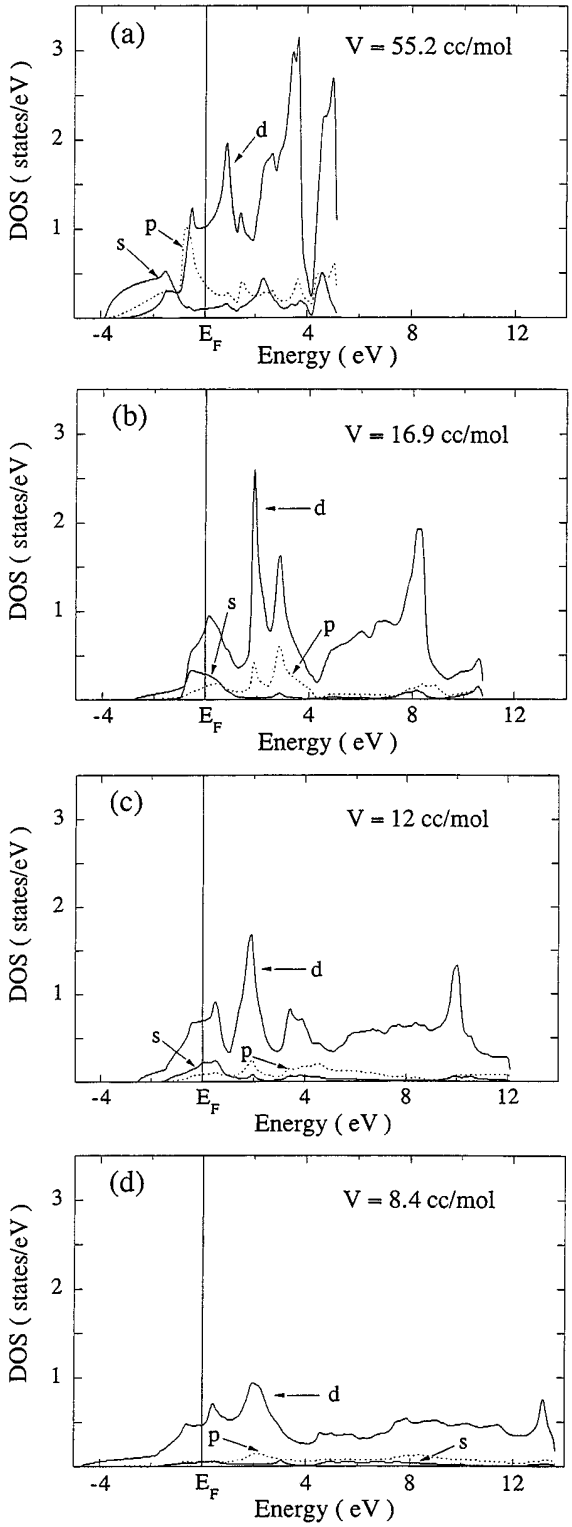

Figure 3. Calculated electron density of states (DOS) for bcc rubidium at the volumes indicated. The Fermi energy, E_F, is set to 0 eV.

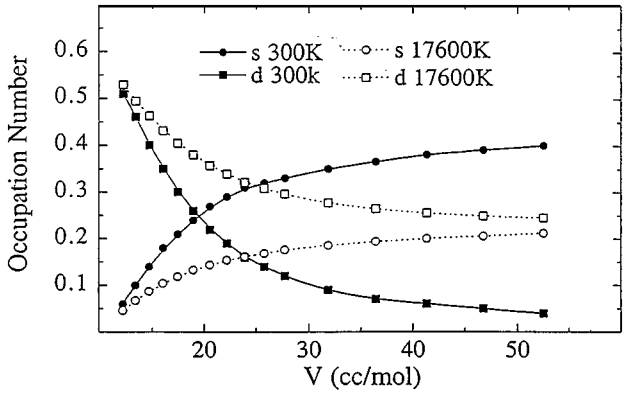

Figure 4. The effect of both compression and temperature on the electron on the s and d occupation number. d occupation increases at the expense of the s electrons with increasing compression. The effect of the higher temperatures is to transfer s electrons to d states for all but the most compressed volumes where the temperature effect diminishes.

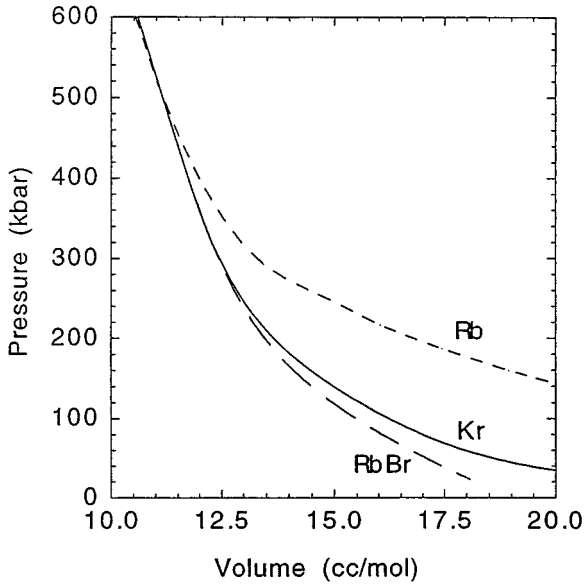

Figure 5. Room temperature isotherms for Kr, RbBr [16] and Rb.

At ambient conditions the electrons making up the Rb 4p inner-core closed shell are widely separated and make a narrow band, but with increasing compression core–core repulsions begin to dominate the pressure. Evidence for the latter can be drawn from the present band calculations which show a broadening of the filled 4p band, but is more vividly displayed in figure 5 by the comparison of room temperature isotherms for Kr, RbBr [16] and Rb. Kr and RbBr are isoelectronic insulating materials in which the highest occupied states are filled 4p bands. The figure shows that near 400 kbar the isotherms of the three materials converge. A similar behaviour has been observed in the case of Cs, Xe and CsI where isotherms of the three materials were found to converge near 100 kbar [17, 18], the limit of the s–d transition in Cs.

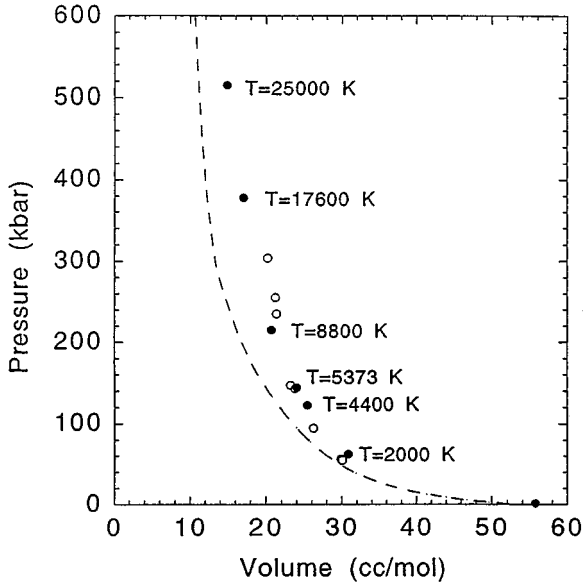

Figure 6. Rb Hugoniots and isotherm. Full circles with temperatures adjacent are from the present calculations. Open circles are data of Rice [8]. The dashed curve is the 0 K FP-LMTO isotherm.

3. Results

Figure 6 shows the experimental Hugoniot [8] and the Hugoniot calculated for rubidium starting from the initial conditions $V_0 = 55.7\ \mathrm{cm}^3\ \mathrm{mol}^{-1}$, $P_0 = 0.00$ kbar and $T_0 = 300$ K. Included in this figure are the $T = 0$ K FP-LMTO isotherm and calculated shock temperatures at several points. The predicted Hugoniot is in good agreement with the data of Rice [8].

The calculated values for the nuclear and electronic gammas along the Hugoniot are plotted in figure 7. At ambient conditions the value of the Slater nuclear gamma is 1.79. It decreases continuously with increasing compression and approaches the limiting value of 0.5 predicted for a system of ions in an electron background [19, 20]. For comparison, calculations made for the Dugdale–McDonald (DM) equation [21] predict a smaller gamma at ambient conditions but follow the Slater values closely for the range of volumes attained by the experimental measurements which is from 30 to 16 $\mathrm{cm}^3\ \mathrm{mol}^{-1}$. The fact that both models converge at high compression and to the correct limiting values suggests that choosing between currently available nuclear models is unlikely to alter matters significantly.

The electronic Grüneisen parameter is defined as $\gamma_{el} = V(\partial P_{el}/\partial E_{el})_v$, in analogy with the nuclear parameter. It can also be written in terms of the temperature as $\gamma_{el} = (V/C_{el})(\partial P_{el}/\partial T)_v$, where C_{el} is the constant volume electronic heat capacity. γ_{el} has a value of -0.3 at ambient conditions due to the pressure lowering resulting from thermal electronic excitation to d states from the more repulsive s states. With decreasing volume γ_{el} decreases slowly and reaches a minimum value at 16 $\mathrm{cm}^3\ \mathrm{mol}^{-1}$. At this volume the transfer has begun to saturate and with increasing temperature γ_{el} begins to approach the limiting high temperature value of two-thirds for an electron gas.

The partly cancelling effect of γ_n and γ_{el} is to reduce the influence of thermal contributions and as a consequence the Hugoniot and isothermal pressure are relatively close together and rise in parallel. The Hugoniot is expected to stiffen above 500 kbar due to the termination of the s–d transition and the overlap of the rare-gas cores.

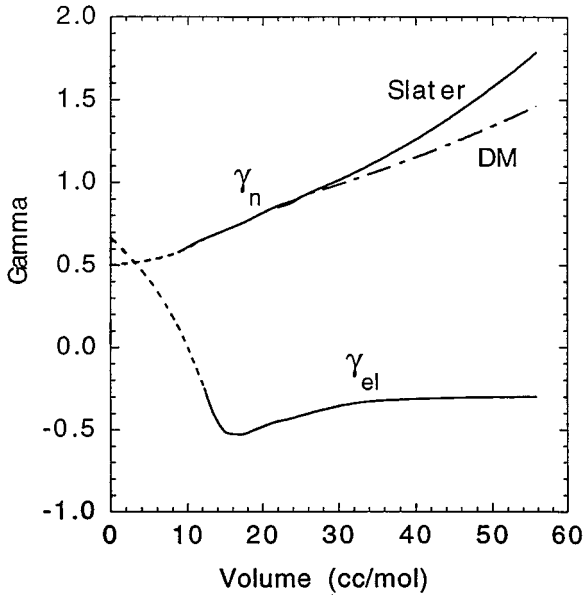

Figure 7. Nuclear and electronic gammas calculated along the Hugoniot.

A detailed comparison of shock wave and static compression data for the alkali metals was undertaken by Grover *et al* [21]. They used the Grüneisen model with the Dugdale–McDonald model for the nuclear thermal contributions, γ_n, but they neglected electronic excitations. In other words their expressions for energy and pressure became

$$E(T, V) = E^*(0, V) + 3NkT \tag{4}$$

and

$$P(V, T) = P^*(0, V) + 3\gamma_n NkT/V. \tag{5}$$

The starred variables (our designation) represent the static lattice energy and pressure at 0 K. The work of Grover *et al* is the inverse of ours: we predict the Hugoniot from calculated isotherms while they determined the 0 K isotherm by fitting the Hugoniot to the shock-wave data. This provides for an interesting comparison.

The reduction of the shock data by Grover *et al* led to a prediction for a temperature isotherm that was significantly lower in pressure than was measured statically by Bridgman [22]. However, subsequent studies have confirmed the correctness of Bridgman's results [15, 23]. The reason for this discrepancy is the explicit neglect of thermal electron excitation.

Figure 8 shows the shock data of Rice, the Hugoniot fit to this data by Grover *et al* and the P^* isotherm that was obtained as a result of this fit. Also included in the figure are the FP-LMTO isotherms at $T = 0$ and 17 600 K. The close agreement of the 17 600 K isotherm with Grover's prediction shows that E^* and P^* should be identified with the $E_{el}(T, V)$ and $P_{el}(T, V)$ in equations (2) and (3). By fitting the Hugoniot they extracted an isotherm that included thermal electron effects.

Figure 9 shows that the predicted shock temperatures calculated with the present model are consistently lower than those predicted by Grover *et al* , because when electron effects are included in the calculations they act as an energy sink that reduces the temperature rise. At 300 kbar our predicted Hugoniot temperature is 13 000 K, or about 5000 K lower. These results

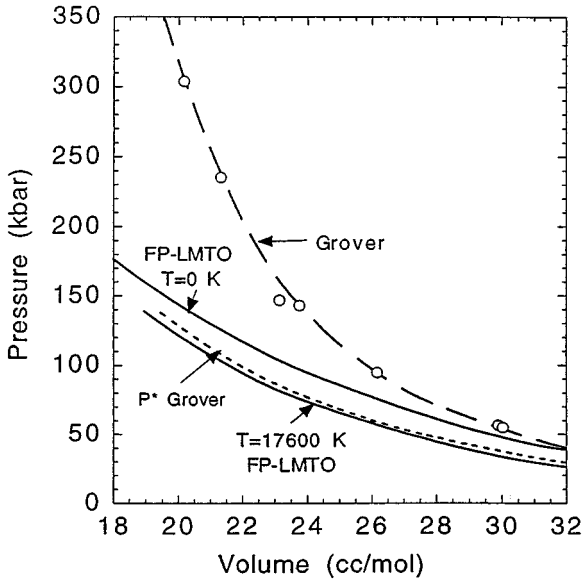

Figure 8. Comparison of shock data and isotherms. Open circles are the shock data [8], and the long-dashed curve is fitted to this Hugoniot by Grover *et al* [21]. The P^* (short-dashed curves) is the isotherm obtained from this fit. Also included for comparison are the FP-LMTO isotherms at $T = 0$ and 17 600 K.

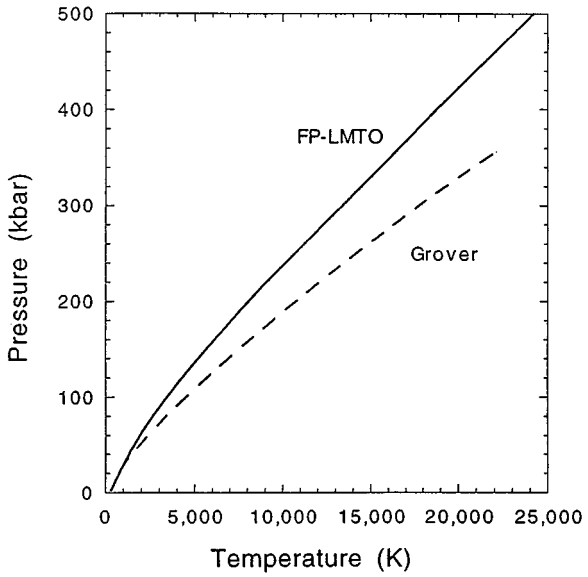

Figure 9. Calculated Hugoniot temperatures versus pressure.

confirm the importance of including the thermal electron effects in calculating the equation of state. Grover, in a subsequent paper, acknowledged the likely importance of d electrons but without introducing further calculations [24].

4. Discussion

While the maximum pressure of 300 kbar reached experimentally for Rb is not particularly high for a shock-compressed metal, the degree of compression up to $V_0/V \sim 2.8$ at a temperature of ∼13 000 K is relatively high. New experiments with rubidium, using present day techniques, could extend the P–T range considerably higher and provide important data for testing theoretical models of dense partially degenerate metals and plasmas. However, the present study suggests that theoretical closure may not be achieved without including shock temperature measurements.

To summarize, we have calculated the static and shock equation of state for Rb in very good agreement with experiment. By comparing our results with previous theory [21] we conclude that it is necessary to take electronic thermal excitation into account in order to accurately describe shock-compressed Rb. The equation of state of Rb is governed by changes of the electronic structure induced by the compression and the increase in temperature, namely, the pressure-induced lowering of the s band compared to the d band and the thermal transfer of s electrons into bonding d states, thereby reducing the shock pressure.

Acknowledgments

The work was performed under the auspices of the US Department of Energy by the Lawrence Livermore National Laboratory under contract No W-7405-ENG-48.

References

[1] Skriver H L 1985 *Phys. Rev.* B **31** 1909
[2] Grosshans W A and Holzapfel W B 1992 *Phys. Rev.* B **45** 5171
[3] Duthie J C and Pettifor D G 1977 *Phys. Rev. Lett.* **38** 564
[4] Rice M H, McQueen R G and Walsh J M 1958 *Compression of Solids by Strong Shock Waves (Solid State Physics 6)* ed F Sietz and D Turnbull (New York: Academic) pp 1–63
[5] Boehler R and Zha C-S 1986 *Physica* B **139/140** 233
[6] Schwarz U, Takemura K, Hanfland M and Syassen K 1998 *Phys. Rev. Lett.* **81** 2711
[7] Brown J M and McQueen R G 1986 *J. Geophys. Res.* **91** 7485
[8] Rice M H 1965 *J. Phys. Chem. Solids* **26** 483
[9] Born M and Huang K 1956 *Dynamical Theory of Crystal Lattices* (Oxford: Oxford University Press)
[10] Hord L B, McMahan A K and Ross M 1977 *Phys. Rev.* B **15** 726
[11] Slater J C 1939 *Introduction to Chemical Physics* (New York: McGraw-Hill)
[12] Perdew J P, Chevery J A, Vosko S H, Jackson K A, Pederson M R and Singh P J 1992 *Phys. Rev.* B **46** 6671
[13] Söderlind P, Moriarty J A and Wills J M 1996 *Phys. Rev.* B **53** 14 063
[14] Murnaghan F D 1944 *Proc. Natl Adac. Sci. USA* **30** 244
[15] Winzenick M, Vijayakumar V and Holzapfel W B 1994 *Phys. Rev.* B **50** 12 381
[16] Aleksandrov L V, Zisman A N and Stishov S M 1987 *Sov. Phys.–JETP* **65** 372
[17] Zisman N, Aleksandrov L V and Stishov S M 1985 *Phys. Rev.* B **32** 484
[18] Takemura K, Shimomura O and Fujihiso H 1991 *Phys. Rev. Lett.* **66** 2014
[19] Kopyshev V P 1965 *Sov. Phys.–Dokl.* **10** 338
[20] Holt A C and Ross M 1970 *Phys. Rev.* B **1** 2700
[21] Grover R, Keeler R N, Rogers F J and Kennedy G C 1969 *J. Phys. Chem. Solids* **30** 2091
[22] Bridgman P W 1947 *Proc. Am. Acad. Arts Sci.* **76** 55
[23] Takemura K and Syassen K 1982 *Solid State Commun.* **44** 1161
[24] Grover R 1971 *J. Phys. Chem. Solids* **32** 2539